Vol. 43, No. 2 (2021) 177-188, DOI: 10.24874/ti.906.06.20.11

Tribology in Industry

www.tribology.rs

RESEARCH

Influence of Welding Position on Tribological Behavior of SS-309L Cladded Surface on 9Cr-1Mo Steel

V.D. Kalyankar[a], H.V. Naik[a,*]

[a]*Sardar Vallabhbhai National Institute of Technology, Surat-395007, Gujarat, India.*

Keywords:

9Cr-1Mo steel
SS-309L
Flux cored arc welding (FCAW)
Welding position
Abrasive wear
Dilution
SEM
EDS

* Corresponding author:

Hardik Vijaykumar Naik
E-mail: naik.hardik.v@gmail.com

Received: 16 June 2020
Revised: 9 September 2020
Accepted: 6 November 2020

A B S T R A C T

Welding position is a significant parameter for weld hardfacing operations applicable to engineering valves, coal transmission pipes in thermal power plants, mining industries, etc. Weld deposition is conducted with horizontal (1G) and vertical (3G) positions due to appropriate orientation of various engineering products. However, parameters like current, speed, travel angle, etc. are different for both welding positions. Therefore, it is required to investigate the influence of these two welding positions on tribological characteristics. In the present work, 1G and 3G weld positions are considered for SS-309L weld hardfacing on 9Cr-1Mo substrate material using flux cored arc welding (FCAW) process. Weld deposited surfaces are subjected to essential mechanical and metallurgical characterizations. Results confirm that the surface deposited using 1G position has higher slurry abrasive wear resistance (0.036 gms), lower dilution (14 %), and lower heat affected zone (HAZ) width (1.5 mm) which is significantly better than 3G position. SEM analysis shows fine elongated grains which precipitate from Cr element as nucleation site for the growth resulting in an improved eutectic matrix within fine grain structure. Wear resistance is improved in 1G position due to uniform elemental distribution of Fe and Cr observed with EDS analysis. Hence, 1G position is the best suitable position for weld hardfacing operations.

1. INTRODUCTION

Creep resistant 9-12 % chromium (Cr) steels are commonly used to manufacture a high temperature steam pipes and the engineering valves applications in ultra-critical and super critical thermal power plants [1]. Some of the typical applications of this also include in power generation industry and in components like thermal shield, valves, boilers, steam pipes, turbine blades and tubes [2,3]. Amongst these components, the engineering valves and the coal carrying pipes require hardfacing of superficial alloys in order to increase the abrasive wear resistance and service lifespan. Furthermore, slurry abrasive wear caused by contact has been a matter of significant consideration amongst researchers due to the intensity of the damages

and the long-distance pipe lines used for coal transportation in power generation industry. Out of 9-12% Cr steels, 9Cr-1Mo steels are extensively chosen material to manufacture pipe components, valves, discs in power plant industries [3-5]. Amongst these components, engineering valves and coal carrying pipes are greatly exposed to abrasive wear during service conditions because of sliding contacts between two metals. Hence, it is necessary to conduct weld hardfacing/weld overlapping on 9Cr-1Mo steels in order to increase abrasive wear resistance. Laser cladding, plasma transferred arc (PTA), flux cored arc welding (FCAW), thermal spray techniques, and gas metal arc welding (GMAW) have been commonly used weld overlapping technique for hardfacing [3-5]. For engineering valves and coal carrying pipes, Co based and Ni based hardfacing materials are commonly observed as weld overlay material which are deposited by PTA technique on 9Cr-1Mo steels [2-5]. Delamination and cracks are witnessed during service conditions for direct deposition of hardfacing materials on 9Cr-1Mo steel [2]. In order to prevent delamination, soft eutectic matrix was recommended before weld hardfacing on 9Cr-1Mo steels as substrate material [2]. Therefore, austenitic stainless steels are recommended as buffer layer material to be deposited in between hardfacing material and 9Cr-1Mo steels to prevent any possible delamination failure [2,3]. FCAW process has been widely used for weld deposition of buffer layer in industries due to minimal dilution of Fe and lower HAZ width [2,3].

For hardfacing operations, current, travel speed, oscillation width, welding position, and standoff distance are significant parameters. However, amongst all these parameters, very few studies have been undertaken to study the welding position. Tribological properties of any weld deposited surface is affected by heat input and elemental dilution. Welding position affects mainly elemental dilution of weld deposited surface owing to varied heat input. Hence, welding position is one of the essential parameters considering weld hardfacing operations for engineering valves and coal carrying pipes in power plant industries. Furthermore, the manufacturing industries follow standard guidelines in hardfacing operations on engineering valves and coal transmission pipelines as per ASME section-IX [6]. As per ASME section-IX, welding position is considered as an essential variable for hardfacing and weld deposition operations. There are six diverse groove positions for welding operations and five fillet positions for different welding processes. Fillet weld position varies from 1F to 5F and these weld positions are not used in hardfacing operations. Further, there are 1G to 6G weld position and 2G, 4G, 5G and 6G weld positions are used for joining application due to mentioned orientation of said weld positions. Hence, recommended welding positions are flat position (1G) and vertical position (3G) for hardfacing operations. Hence, these two welding positions have been considered in this present experimental investigation. According to ASM handbook, form of hardfacing material, cost of material, deposition rate, workpiece characteristics, deposition thickness, and dilution rate are considered aspects to establish welding procedure for components [7]. Amongst them, welding dilution causes the change in the elemental composition of hardfacing material due to the admixture of deposition material and substrate material [7,8]. Current and travel speed are an important process parameter which affect the dilution in hardfacing operation [8]. Parameters like current, travel speed, feed rate are different for 1G and 3G positions due to variance in orientation of substrate material and capillary action of molten pool. The values of heat input and current are different for 1G and 3G welding positions. Since, welding position has direct relation with current and heat input, this work has been focused on studying effect of welding position. Moreover, current and heat input also depend upon material composition and weld deposition procedure. Hence, it is important to study welding position for particular set of materials and methods.

Welding position affects mainly heat input which is the most significant factor during any hardfacing operation since it directly affects the welding dilution. Many previous studies show the influence of heat input on dilution and wear resistance [9,10]. Zhao et al. [11] have observed the influence of heat input on the grain size and hardness, and have found that higher hardness could be resulted due to finer grain size. The higher values of current lead to ease out distribution of elements such as Fe and Cr from the substrate to the weld deposition layer and

hence, it results in the lower wear resistance and the higher welding dilution [12,13]. The lower wear resistance of coating is observed at higher heat input due to the formation of hypoeutectic microstructure thereby forming interdendritic eutectic lamellar structure and cobalt solid solution dendrites [14]. Hence, it is important to establish the best suitable welding position for different components since welding position directly affects dilution. This established welding position can be used as a futuristic consideration in the steam turbine components for hardfacing operations. However, this requires a significant experimental investigations and observations on the abrasive wear resistance as well as the hardness recommend either to 1G or to 3G welding positions. The present research work aims to study the influence of these essential welding positions i.e. of 1G and of 3G on the tribological properties. In this work, the influence of welding position has been investigated for a buffer layer application i.e. the deposition of austenitic materials.

The primary objective of this research study is to understand the influence of welding positions on the weld deposition characteristics on 9Cr-1Mo steels. Therefore, the weld deposition material and the process selected have been based on a buffer layer application and the industrial requirements taken from M/S L&T MHPS Turbine Generators Pvt. Ltd., Hazira, Gujarat, India. Furthermore, FCAW process has been considered as a weld deposition method due to a minimum dilution of Fe and lower HAZ hardness [2,3]. Therefore, FCAW process has been investigated for the weld deposition of an austenitic stainless steels on 9Cr-1Mo steels which has been based on industry practice and literature support [2,3]. In the present work, FCAW process has been selected as weld deposition technique and SS-309L austenitic stainless steel as a weld deposition material. An extensive mechanical and microstructural characterization like slurry abrasive wear test, hardness, welding dilution, elemental distribution, microstructural changes have been considered for 1G and for 3G welding positions. The main outcome of this work is to bring out a conclusive remark in accordance with the effect of welding positions on weld deposition characteristics, mechanical and metallurgical characterization in the hardfacing operations. How far the welding position is suitable and influential, has been finalized from a comparative analysis and metallurgical characterizations in the hardfacing operations.

2. MATERIALS AND METHODS

2.1 Substrate and weld deposition material combination

The base material used in the present investigation is in the form of 9Cr-1Mo steel plates of the sizes 200 mm x 100 mm x 14 mm which have been cut from a rolled sheet and the filler is from SS-309L FCAW wire of the size 1.2 mm diameter. For this work, P91 material was provided by M/S L&T MHPS Turbine Generators Pvt. Ltd. and provided P91 material has 450 N / mm^2 yield strength, 180 HV-200 HV hardness and 585 N / mm^2 tensile strength. Table 1 shows the chemical composition of the substrate and the weld overlay material used in this work.

Table 1. Chemical composition (wt.%) of materials under consideration.

Element	**C**	**Cr**	**Mn**	**V**	**Mo**	**Ni**	**Fe**
9Cr-1Mo steel	0.08	8.56	0.39	0.153	0.9	0.25	Bal.
Element	**C**	**Cr**	**Mn**	**S**	**Si**	**Ni**	**Fe**
SS-309L	0.03	23	1.2	0.008	0.5	12.6	Bal.

2.2 Weld deposition method

In this work, several trial runs have been conducted for both the welding positions and for the said material combinations to identify process parameters. This was done before the main experiments in accordance with the literature support and industrial practice [2,3]. All of these experiments have been conducted at M/S L&T MHPS Turbine Generators Pvt. Ltd., Hazira, Gujarat, India by using synergic welding machine (make: Fronius TransSteel 500). Although FCAW method has been used in the manual mode, still utmost attention was paid to the actual weld deposition of material considering skill aspect. Moreover, all the samples were subjected to dye penetration (DP) test in order to examine any surface defect on the substrate material before the weld deposition of SS-309L. Chemical composition was ensured at several points with positive material identification (PMI) machine to confirm the exact chemical composition for 9Cr-1Mo steel. Trial experiments were conducted to

identify process parameters for both the welding positions. After the elimination of possible crack formation during weld deposition over 9Cr-1Mo steel, process parameters were finalized to identify the weld deposition material and the same is depicted in Table 2. For the calculation of heat input per unit length, formula (1) was used.

$$H = (I * V * 0.06) / S \quad (1)$$

Where, H, I, V and S represent the heat input per unit length, welding current, arc voltage and welding speed. SS-309L was the weld deposited with the chosen process parameters on 9Cr-1Mo steels by using FCAW process in 1G and in 3G positions as shown in Fig. 1. However, no surface cracks or welding defects were ensured with the help of DP test.

Table 2. Parameters considered for weld overlay deposition by FCAW process.

Sr. No.	Parameters	Sample codes	
		FCAW-1G (Horizontal position)	FCAW-3G (Vertical position)
1	Current	250 - 270 A	145 - 160 A
2	Voltage	26 - 28 V	19 - 21 V
3	Feed rate	8 mm/min	4.4 mm/min
4	Flow rate	20 l/min	20 l/min
5	Shielding gas pressure	3.5 Mpa	3.5 Mpa
6	Travel speed	6 mm/ sec	0.8 mm/ sec
7	Heat input	1.3-1.4 KJ/ mm	3.8-3.9 KJ/ mm

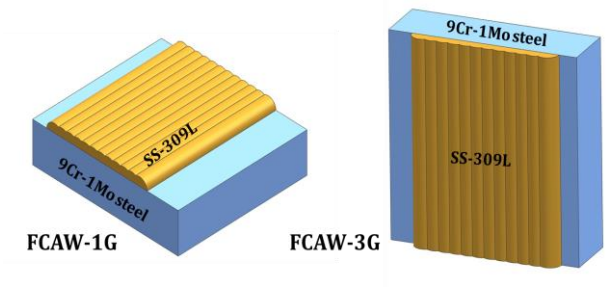

Fig. 1. Representation of welding positions 1G (FCAW-1G) and 3G (FCAW-3G).

Pre-heating at 250 °C and interpass temperature at 315 °C were sustained before and during weld deposition of SS-309L material to avoid any possible crack formation. Samples were cooled down at 100 °C followed by heating up to 400 °C temperature for 60 minutes to remove excess hydrogen. This was taken into consideration for the prevention of hydrogen induced cracking as per dehydrogenation heat treatment (DHT) [3]. DHT reduced the chances of hydrogen-induced crack formation after the weld deposition of SS-309L material. Hence, all the samples were ensured crack-free for both the welding positions. Further, 1G and 3G samples were subjected in stress relieving post weld heat treatment (PWHT) at 750 °C temperature with soaking time of 60 minutes based on the standard industrial practice and literature support [2,3]. After the successful weld deposition of SS-309L on 9Cr-1Mo steel, samples were considered for in-depth investigation aspects like slurry abrasive wear test, microhardness, dilution, metallurgical bonding, and microstructural analysis of cladded surface obtained with 1G and 3G positions.

2.3 Characterization methods

Coal carrying pipes and engineering valves components are exposed to severe working conditions like flow of coal, ash particles, high temperature chemical exposure, flow at high velocity, etc. are usually subjected to abrasion and wear [3]. For the measurement of welding dilution, multi-track specimen was transversely sectioned on abrasive cutting machine. Afterwards, it was polished on different girt of emery papers followed by chemical etching and Viella's (5 cc HCL + 2 gms Picric acid + 100 cc Ethyl alcohol) etchant (4 mins) was used for the same as per the ASTM E407 standard [15]. Samples were then analyzed in vision measuring system (make: Rapid I V 2015 J LX). After obtaining this image, the analysis part was done in AutoCAD software for measurement of deposited area (A) and diluted area (B) for the calculations based on formula (2), where D is welding dilution.

$$D = \frac{B \cdot 100\ \%}{A + B} \quad (2)$$

In order to observe the microstructural changes corresponding to each welding position combination, samples were machined perpendicular to weld deposition direction. Samples were prepared in accordance with ASTM E407 [15] for metallographic studies. Further, samples were etched chemically with Viella's (5 cc HCL + 2 gms Picric acid + 100 cc Ethyl alcohol) etchant (4 mins) for 1G and for 3G samples. Different metallurgical zones of interest like weld deposited coating, interface and HAZ region under different welding positions were observed with an optical microscope coupled with an image analyzing software. Amongst 1G and 3G samples, sample

with a good mechanical result was analyzed by using scanning electron microscopy (SEM) and energy dispersive spectroscopy (EDS) to identify reasons behind an improved result. SEM and EDS analysis are useful in order to determine in depth justification for an improved mechanical result. Microstructural characterization is discussed for both the positions in section 3.

Vickers microhardness testing machine (make: HM-211-Mitutoyo Corporation) was considered to measure microhardness for 1G and for 3G welding positions individually. Test parameters were taken at testing load of 1000 gf having dwell time of 10 seconds for all indentations [2]. There were few indentations taken at uniform distance and average hardness was recorded for comparison. Different abrasion and wear conditions are analysed and tested as per the ASTM standards. Slurry abrasion wear test was selected for this research work and same was conducted as per the ASTM G105 [16]. Experimental set up (make: Ducom instruments) for the same has been presented in Fig. 2 for the said test.

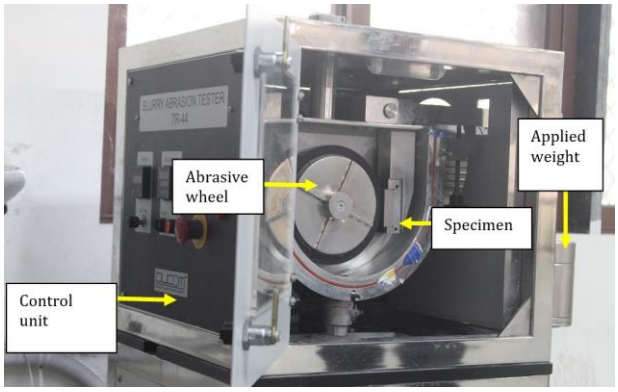

Fig. 2. Set up used for the slurry abrasive wear test.

Test parameters and required specimen (rectangular, flat in shape with the size of 25.4 ±0.8 mm wide, 57.2 ±0.8 mm long and 6.4 to 15.9 mm thickness) were machined in accordance with the requirement of ASTM G105 [16]. For this work, ASTM G105 standard was followed for selecting test parameters. For this test, test time (1000 revolutions) and RPM (245 rpm) were maintained according to ASTM G105. Specimen' surface finish of about 0.5 to 0.75 μm was achieved by surface grinding and polishing with successive grit of emery papers. For this work, slurry abrasive wear was measured in terms of weight loss and obtained results are discussed in section 3.

3. RESULTS AND DISCUSSION

3.1 Weld deposition characteristics

FCAW process has been applied in two different welding positions as mentioned earlier. In cladding operation, short circuit transfer mode has been observed in FCAW process. In this work, same mode has been maintained for both welding positions due to less spatter and good mechanical properties. The weld bead characteristics were analysed in terms of appearance, uniform external surface and obtained coating thickness. After the weld deposition in both the welding positions, weld bead characteristics of obtained surface is presented in Figs. 3a. and 3b.

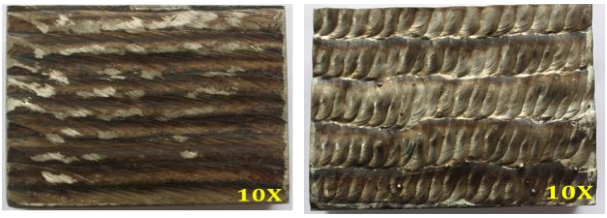

(a) (b)

Fig. 3. FCAW process sample (a) 1G position, (b) 3G position.

As is shown in Fig. 3a, visual observation has confirmed the uniformity and less spatter for 1G position. Whereas, non-uniformity and waviness were observed in 3G position (Fig. 3b) mainly due to higher heat input per unit length and gravitational force which resulted in increment in size of molten pool and fall of the molten pool at given instant. Coating thickness was measured with optical microscope and in-built ruler and coating thickness was observed around 6-8 mm in the case of 3G position whereas, 4-5 mm coating thickness was obsered in 1G position. Higher coating thickness was observed in 3G position due to non-uniform bead characteristics and overlapping of weld deposition layer. This leads to a conclusion for hardfacing application that 1G can be recommended welding position mainly due to uniform external surface along with required minimum coating thickness as 3G position leads to wastage of excess material.

3.2 Weld dilution

Welding dilution has a significant impact on the wear resistance of hardfacing material [3,8,17].

1G and 3G samples were machined and etched as per the standard procedure. Images of samples had been captured with vision measuring system (make: Rapid I V 2015 J LX). These images (magnification: 10X) were exported to AutoCAD software followed by ImageJ software for analysis purpose. In this work, images of FCAW-1G and FCAW-3G samples are represented in Figs. 4 and 5 respectively.

After obtaining this image, the analysis part was done in ImageJ software for measurement of deposited area and diluted area for the calculations. Where, B is re-melted diluted area and A is the weld overlay cross-section area as is shown in Figs. 4 and 5. For this work, welding dilution was observed around 14 % for FCAW-1G and around 24 % for FCAW-3G position. The significant reduction in 1G samples was due to less current value during weld deposition. Diffusion of substrate material and hardfacing were less in 1G samples and re-melting of 9Cr-1Mo steel was less in 1G samples. Hence, improved mechanical characteristics were observed in 1G samples which make this position as a suitable welding position for hardfacing method. Improved mechanical properties were obtained due to less dilution Fe in coating material leading to different microstructure that produces good hardness in 1G position.

3.3 Elemental distribution

EDS specimen was prepared as per standard metallographic method and the same was etched with the above-mentioned etchant. The steps for microstructural observations and sample preparation are kept as per standard metallographic method. In this analysis, EDS line scan analysis, as shown in Fig. 6, has been chosen to study an elemental distribution amongst different regions like coating, interface and substrate for SS-309L material.

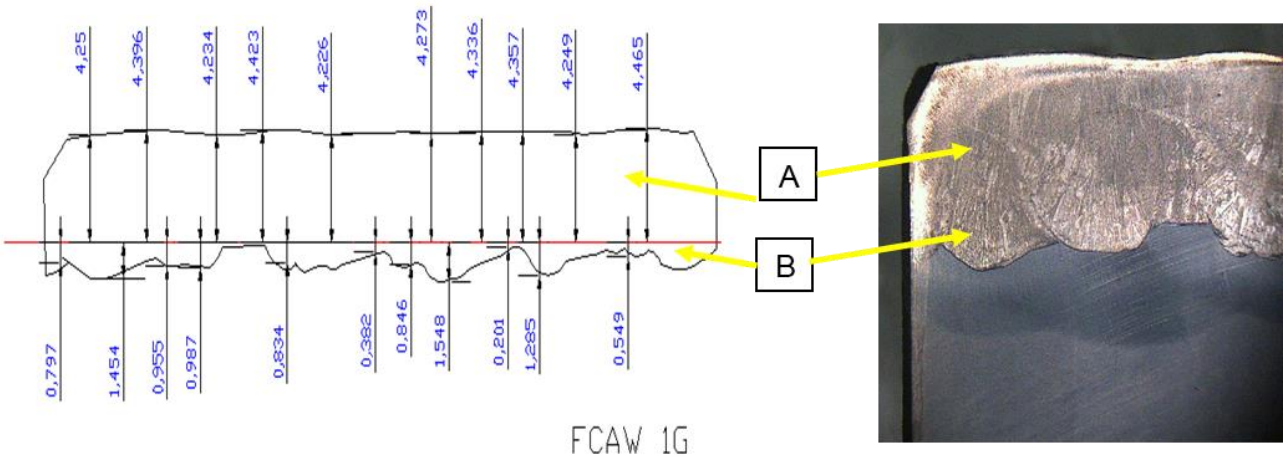

Fig. 4. Welding dilution of overlay surface obtained by 1G position.

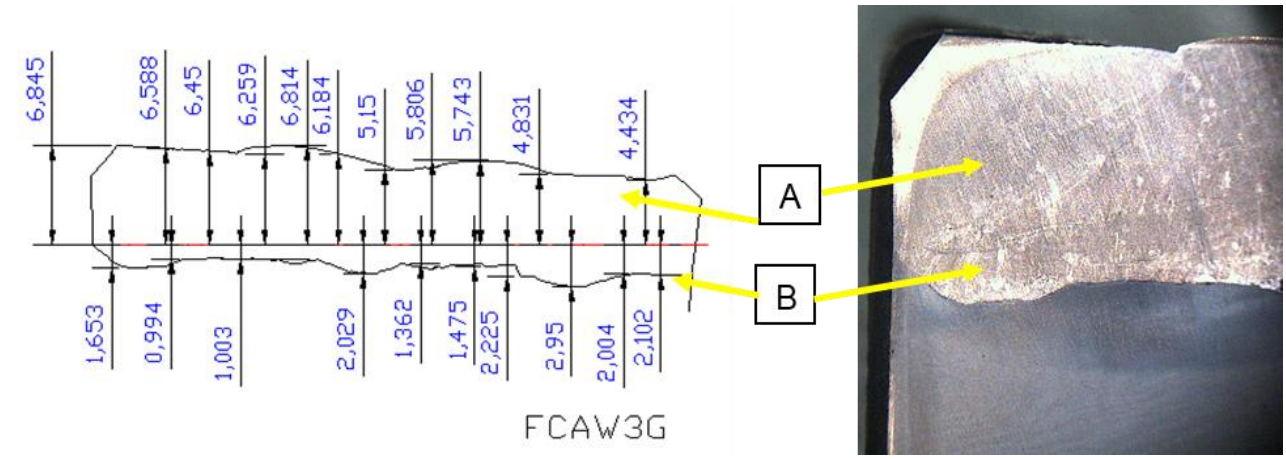

Fig. 5. Welding dilution of overlay surface obtained by 3G position.

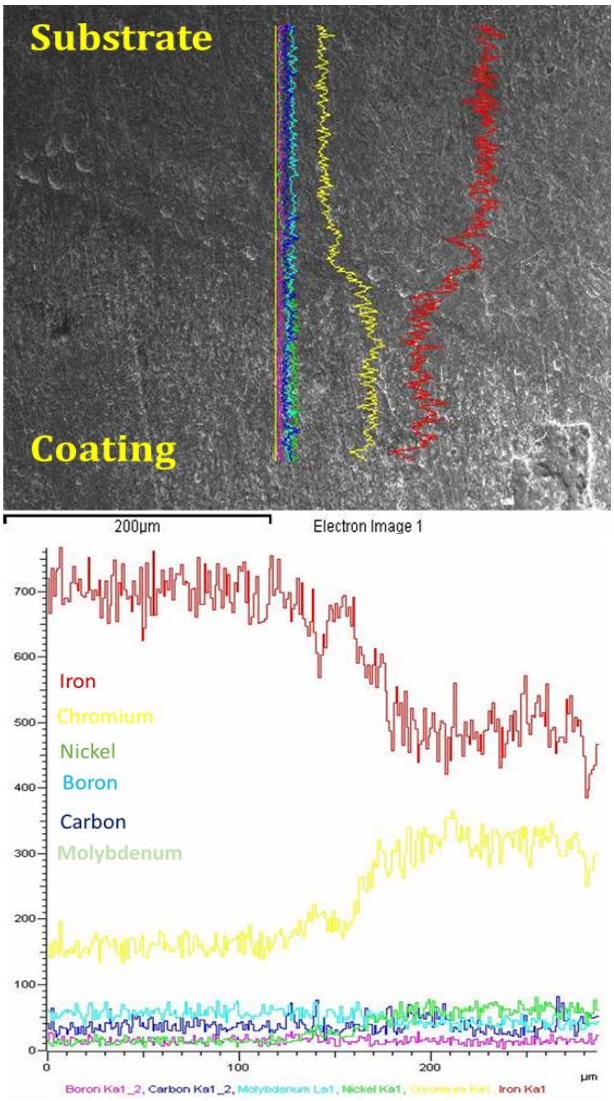

Fig. 6. EDS line scan analysis of 1G position sample.

As is shown in Fig. 6, Fe and Cr were core content elements for analysis since Fe content affects the outcomes of hardness and wear resistance [17,18] and Cr content affects the outcomes of sensitization that takes place during service conditions by Cr precipitation. The result proves that, Hardness could be witnessed on higher side in coating region due to decreased level of Fe content in fusion and coating zone. On the other hand, Cr content increases in coating region and near fusion line, it is seen with similar content as Fe content. Even, carbon mitigation is seen very less which reduces the chances of cracks in fusion line as DHT is applied after weld overlay.

3.4 Microstructural characterization

Mechanical properties are the function of metallurgical changes that occur during and after weld deposition process. Specimen from 1G and from 3G position samples were machined as per the requirement of microstructural analysis. Both the samples were subjected to optical microscope for microstructural changes after chemical etching. Figure 7 represents the microstructural images of coating material's region that was captured through optical microscope at magnification of 200x.

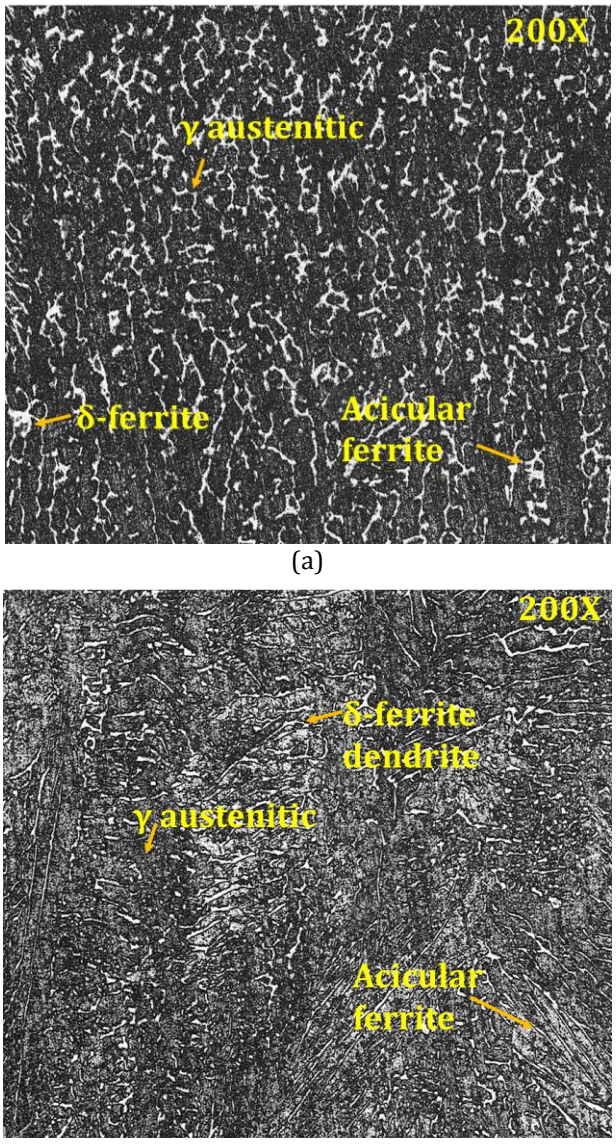

Fig. 7. Optical micrographs of coating region (a) FCAW-1G (b) FCAW-3G.

Microstructural images of both the welding positions for SS-309L coating material are represented in Figs. 7a and 7b for 1G and for 3G positions respectively. Figure 7a even represents the uniform and fine elongated grain structure for 1G welding position. Fine elongated grains were observed due to precipitation from Cr element

which acts as a nucleation site for the growth. This nucleation growth has helped in formation of an improved eutectic matrix within fine grain structure. The growth of this eutectic structure is due to difference in solidification parameter G/R (G – temperature gradient; R–rate of solidification) and heterogeneous nucleation at P91 steel surface [19]. In 3G position, volume fraction of acicular ferrite is more than 1G position. Hence, hardness was observed less in 3G position in coating region. Acicular formation and delta ferrite formation were observed on lower volume fraction due to faster cooling and higher G/R ratio which leads to higher hardness and less crack chances in 1G position. However, similar microstructure and phase morphology was observed in 1G and 3G position due to similar process and material combination [19,20]. Whereas, in Fig. 9b coarser grain patches are observed with elongated grains. There are few microcracks observed in weld overlay zone as it was difficult to accommodate proper shielding during deposition of SS-309L weld overlay material in vertical uphill position. As the main purpose of this work is to study the influence of welding position on the uniformity of grain structure, which has been clearly observed in welding position 1G. The main reason behind this observation was due to less heat input and against gravitational force/capillary action during overlay approach in 1G position.

From the comparative analysis, 1G position sample has been considered for further analysis in terms of SEM and EDS in order to understand microstructural changes occurred after application of SS-309L material. SEM-EDS specimen were prepared according to standard metallographic method and same was etched with same etchant. Steps for microstructural observations and sample preparation are as per the standard metallographic method. Sufficient evidences prove that the best welding position is 1G position. Hence, FCAW -1G position has been considered for SEM-EDS analysis for in depth microstructural characterization.

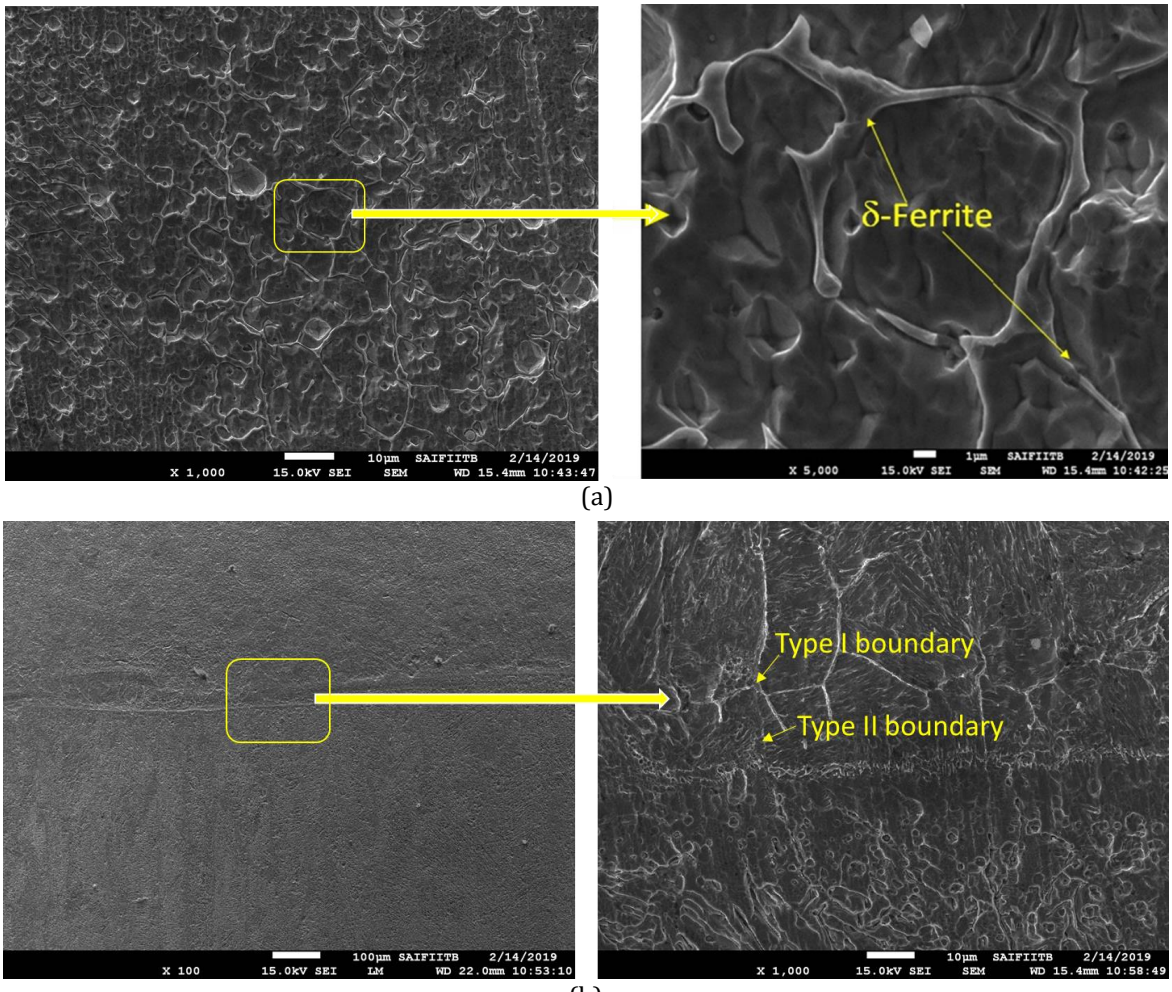

(a)

(b)

Fig. 8. SEM micrographs of 1G position sample (a) coating region, (b) interface region.

In this work, 1G position specimen was subjected to SEM (make: JEOL -JSM-7600F, Japan) for microstructural analysis purpose. Microstructural images of coating and interface region are represented in Figs. 8a and 8b respectively captured from SEM at different magnifications which are mentioned in micrographs. SEM micrographs of coating material (SS-309L) is shown in Fig. 8a which represents the uniform and fine elongated grain structure. It is observed that fine elongated grains are precipitated from Cr element as a nucleation site for the growth which resulted in an improved eutectic matrix within fine grain structure.

Whereas, in Fig. 8b coarser grain patches are displayed with elongated grains. There are two types of grain boundaries seen near the fusion line which are categorized as Type I and Type II boundary. At the interface, microstructure was observed with typical sandwich structure containing a white bright band ended with multi micro-voids type-II boundary. FCAW-1G sample analysis showed less element changes near type-II boundary. Hence, less elemental change near type-I and type-II boundaries have affected less to weld property. For FCAW-1G position, type-II boundary was observed less and hence, it helps in less variation in hardness. Further, delta ferrite phase is seen in austenite matrix in this micrograph represented in Fig. 8a. There are no microcracks observed in weld overlay zone as DHT treatment was implemented after weld overlay application. Fine and uniform grain structure has been obtained without residual stress in HAZ with use of PWHT. Grain refinement has been observed in SS-309L material with application of PWHT in FCAW-1G position samples.

3.5 HAZ width

HAZ has been considered a significant aspect for any welding process since heat input directly affects this region. Varying heat input in accordance with two different welding positions has been considered for this work. Optical micrographs at the interface were taken for both welding positions to observe HAZ in substrate region. It is desirable to have small HAZ width for 9Cr-1Mo steels to reduce the chances of martensite formation during service conditions.

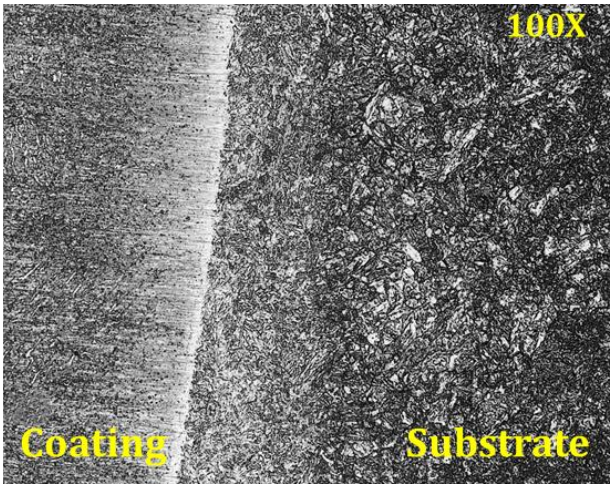

(a)

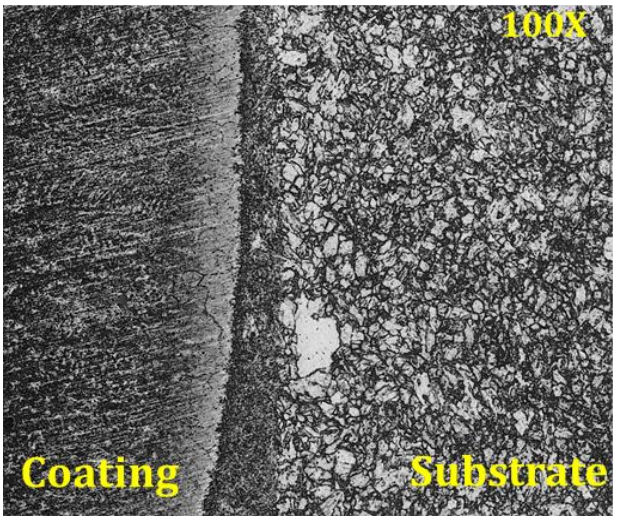

(b)

Fig. 9. Optical microstructure images of interface region (a) 1G sample, (b) 3G sample.

Figure 9a represents coating region, HAZ and substrate region for the sample obtained with 1G position. This micrograph was taken at 100X in order to observe HAZ width and microstructural changes at the interface region of 1G position. HAZ width was measured by an inbuilt ruler and it was observed around 1.5 to 2 mm. Same approach has been adopted to take image from another sample which is obtained with 3G position. Figure 9b shows the representation of microstructural image that involves in coating region, HAZ and substrate region of 3G sample. HAZ width was measured around 2 to 2.5 mm. The width of HAZ should be as much minimum as possible to avoid crack formation in 9Cr-1Mo material which is highly sensitive material at elevated temperature and varying temperature gradient. Residual stresses can be generated during welding operation with the sudden change of heating and cooling. So, the

higher HAZ size in substrate material may result in brittleness and therefore, stress accommodation can be very difficult and it results in cracks at that end [2,4]. Therefore, it is for these reasons that 1G position may act as the suitable welding position for 9Cr-1Mo steels.

3.6 Microhardness

After preparing the samples for two welding positions, microhardness test was conducted for both the samples individually. Fig. 10 shows the comparison between various zones categorized in three regions namely coating, interface and substrate for two samples.

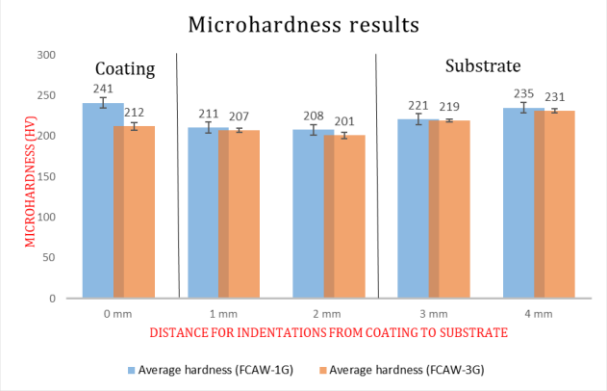

Fig. 10. Hardness obtained across various regions of FCAW-1G and FCAW-3G.

SS-309L is recommend material for developing buffer layer between hardfacing and substrate materials in industry [2,3]. Buffer layer was intended to develop soft matrix in order to prevent any delamination between hardfacing and substrate [3]. This work has been focused to study effect of welding position on tribological properties in accordance with buffer layer material. Hence, hardness was observed in lower side due to soft matrix developed during weld deposition of an austenitic material. Comparative data has been recorded for both the welding positions to study the influence of the same on hardness. From this study, 1G welding position was observed with uniform higher hardness and uniform deposition characteristics compared to 3G welding position. Increased hardness was observed in 1G position due to less dilution and uniform weld deposition of SS-309L material. Higher dilution of Fe can cause lower hardness and wear resistance [2]. Further, PWHT has relieved the residual stresses available at the interface region. Hence, lower hardness was observed at the interface region. Further, there is negligible difference observed in HAZ region and lower hardness was observed in both positions. Hence, 1G position has been recommended position for the given set of material combination.

3.7 Slurry abrasive wear characteristics

After conducting the wear test for two welding positions, weight loss for all samples were measured with the help of digital weighing scale. Wear resistance in terms of weight loss was calculated in accordance with ASTM G105 as similar approach was adopted by the previous researchers [18,19,21]. Figure 11a shows the wear scar observed after the slurry abrasive wear test for 1G sample which represents less indentation of rubber wheel on the surface. Figure 11b represents the wear scars after wear test for 3G sample which has more depth of indentation due to less hardness of surface.

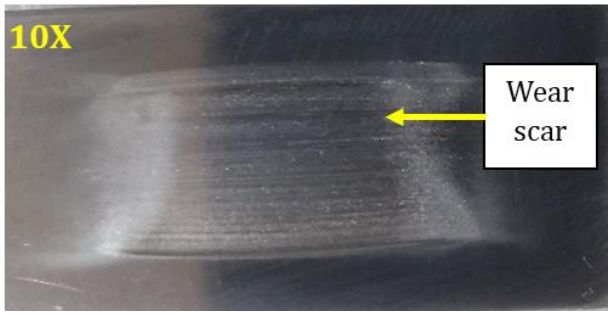

(a)

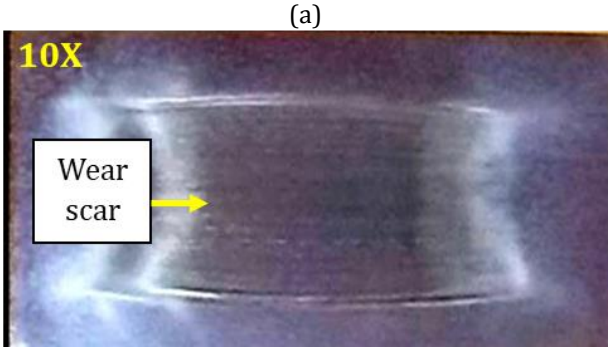

(b)

Fig. 11. Wear scar on (a) FCAW-1G sample (b) FCAW-3G sample.

Weight loss for 1G sample and for 3G sample was observed around 0.036 gms and 0.052 gms respectively. Wear resistance was increased in case of 1G welding position due to less heat input per unit length compared to 3G welding position. During 1G position, heat input per unit length was observed around 1.3 kJ/mm due to chosen current and travel speed. Whereas, higher heat input per unit length was observed

around 3.8 kJ/mm in 3G position. During weld deposition of SS-309L material, travel speed was less in 3G position which produced spatter and non-uniform bead characteristics in 3G samples. Wear resistance has been affected by dilution and hardness of hardfacing materials [2,3]. In this work, lower dilution and higher hardness were observed in 1G position. Further, delta ferrite content which affects the toughness in material has been on lower side for 1G position. Hence, 1G position has been observed with higher wear resistance compared to 3G position. From the literature, abrasive wear with less plastic flow and adhesion was observed. Further, main wear mechanism is abrasive wear with less plastic flow due to detached metal particles [22]. Higher heat input per unit length and higher dilution has caused reduction in wear resistance for 3G position. From these observations, 1G position is recommended for improved wear resistance without any mechanical defects.

4. CONCLUSIONS

SS-309L material has compatibility with 9Cr-1Mo steel in terms of co-efficient of elastic modulus, thermal expansion and melting point which are the significant factors for selecting the weld deposition material. On the basis of experimental investigations and comparative analysis undertaken, the suitability and influence of welding positions are discussed as follows:

- Uniform weld bead and less spatter was observed in 1G position due to less heat input per unit length and absence of gravitational force effect on molten pool. Whereas, non-uniformity and waviness were observed in 3G position.
- Welding dilution was observed around 24 % and 14 % for 3G and 1G welding positions respectively. Diffusion of substrate material and hardfacing were less in 1G samples and re-melting of 9Cr-1Mo steel was less in 1G samples. Hence, improved mechanical characteristics were observed in 1G samples which make this position as a suitable welding position for hardfacing method.
- Microstructural characterisation and elemental analysis showed improved grain orientation and uniform elemental distribution in 1G position. This is due to less heat input per unit length which has resulted in higher solidification G/R ratio.
- Acicular formation and delta ferrite formation were observed on lower volume fraction due to faster cooling and higher G/R ratio which leads to higher hardness and less crack chances in 1G position.
- Due to difference in heat input per unit length, lower wear resistance was observed in 1G position. Further, main wear mechanism was abrasive wear with less plastic flow due to detached metal particles for both positions.

On the basis of investigations, 1G position implemented with FCAW process shows a significant outcome in terms of lower HAZ width, lower dilution and higher slurry abrasive wear resistance. Consequently, it can be said that welding position affects wear resistance, hardness, dilution and HAZ size in hardfacing operations and therefore, on the basis of present investigations, it can be concluded that, 1G welding position is the most suitable position in hardfacing operations due to its improved mechanical and microstructural results.

Acknowledgement

Authors are thankful to M/S L&T MHPS Turbine Generators Pvt. Ltd., Hazira, Gujarat, India, for providing good quality machines, materials and testing facilities to perform the necessary experimental investigations.

REFERENCES

[1] C. Pandey, A. Giri, M.M. Mahapatra, P. Kumar, *Characterization of Microstructure of HAZs in as Welded and Service Condition of P91 Pipe Weldments*, Metals and Materials International, vol. 23, pp. 148-162, 2017, doi: 10.1007/s12540-017-6394-5

[2] H. Kumar, S.K. Albert, C. Sudha, R. Vijayashree, A.K. Bhaduri, C. Balasubramanian, *Hardfacing of a Modified 9Cr–1Mo Steel Component Using a Nickel-Base Alloy*, Transactions of the Indian Institute of Metals, vol. 64, pp. 339-343, 2011, doi: 10.1007/s12666-011-0087-4

[3] M.M. Ferozhkhan, K.G. Kumar, R. Ravibharath, *Metallurgical Study of Stellite 6 Cladding on 309-*

16L Stainless Steel, Arabian Journal for Science and Engineering, vol. 42, pp. 2067-2074, 2017, doi: 10.1007/s13369-017-2457-7

[4] T. Lolla, J. Siefert, S.S. Babu, D. Gandy, *Delamination Failures of Stellite Hardfacing in Power Plants: A Microstructural Characterisation Study*, Science and Technology of Welding and Joining, vol. 19, iss. 6, pp. 476-486, 2014, doi: 10.1179/1362171814Y.0000000213

[5] A.K. Bhaduri, S.K. Albert, C.R. Das, B. Raj, *Hardfacing of Austenitic Stainless Steel with Nickel Base NiCr Alloy*, International Journal of Microstructure and Materials Properties, vol. 6, no. 1-2, pp. 40-53, 2011, doi: 10.1504/IJMMP.2011.040436

[6] ASME Section IX, *Qualification Standard for Welding and Brazing Procedures, Welders, Brazers and Welding and Brazing Operators,* 2017.

[7] S. Kumar, A.S. Shahi, *Effect of Heat Input on the Microstructure and Mechanical Properties of Gas Tungsten Arc Welded AISI 304 Stainless Steel Joints*, Materials & Design, vol. 32, iss. 6, pp. 3617-3623, 2011, doi: 10.1016/j.matdes.2011.02.017

[8] D.D. Deshmukh, V.D. Kalyankar, *Recent Status of Overlay by Plasma Transferred Arc Welding Technique*, International Journal of Materials and Product Technology, vol. 56, no. 1-2, pp. 23-83, 2018, doi: 10.1504/IJMPT.2018.089118

[9] M.A.V. Bermejo, L. Karlsson, L.-E. Svensson, K. Hurtig, H. Rasmuson, M. Frodigh, P. Bengtsson, *Effect of Welding Position on Properties of Duplex and Superduplex Stainless Steel Circumferential Welds*, Welding in the World, vol. 59, pp. 693-703, 2015, doi: 10.1007/s40194-015-0245-0

[10] I.A. Tsibulskiy, M. Kuznetsov, A.D. Akhmetov, *Effect of Welding Position and Gap Between Samples on Hybrid Laser-arc Welding Efficiency*, Applied Mechanics and Materials, vol. 682, pp. 35-40, 2014, doi: 10.4028/www.scientific.net/AMM.682.35

[11] H. Zhao, J. Li, Z. Zheng, A. Wang, D. Zeng, Y. Miao, *The Microstructures and Tribological Properties of Composite Coatings Formed via PTA Surface Alloying of Copper on Nodular Cast Iron*, Surface and Coatings Technology, vol. 286, pp. 303-312, 2016, doi: 10.1016/j.surfcoat.2015.12.037

[12] B. Dikici, S. Ozel, M. Gavgali, I. Somunkiran, *The Effect of Arc Current on the Corrosion Behaviour of Coated NiTi Alloy on AISI304 by Plasma Transferred Arc Process*, Protection of Metals and Physical Chemistry of Surfaces, vol. 48, pp. 563-567, 2012, doi: 10.1134/S2070205112050024

[13] F. Fernandes, A. Ramalho, A. Loureiro, A. Cavaleiro, *Wear Resistance of a Nickel Based Coating Deposited by PTA on Grey Cast Iron*, International Journal of Surface Science and Engineering, vol. 6, no. 3, pp. 201-213, 2012, doi: 10.1504/IJSURFSE.2012.049053

[14] T.J. Antoszczyszyn, R.M.G. Paes, A.S.C.M. D'Oliveira, A. Scheid, *Impact of Dilution on the Microstructure and Properties of Ni-based 625 Alloy Coatings*, Soldagem & Inspecao, vol. 19, no. 2, pp. 134-144, 2014.

[15] ASTM E407-15, *Standard Practice for Microetching Metals and Alloys*, 2015.

[16] ASTM G105-16, *Standard Test Method for Conducting Wet Sand/Rubber Wheel Abrasion Tests*, 2016.

[17] D.D. Deshmukh, V.D. Kalyankar, *Deposition Characteristics of Multitrack Overlay by Plasma Transferred Arc Welding on SS316L with Co-Cr Based Alloy - Influence of Process Parameters*, High Temperature Materials and Processes, vol. 38, iss. 2019, pp. 248-263, 2018, doi: 10.1515/htmp-2018-0046

[18] Z. Feng, M. Tang, Y. Liu, Z. Yan, G. Li, R. Zhang, *In Situ Synthesis of TiC-TiN-Reinforced Fe-base Plasma Cladding Coatings*, Surface Engineering, vol. 34, iss. 4, pp. 309-315, 2018, doi: 10.1080/02670844.2017.1349362

[19] G.A. Rodríguez-Bravo, M. Vite-Torres, J.G. Godinez-Salcedo, *Corrosion Rate and Wear Mechanisms Comparison for AISI 410 Stainless Steel Exposed to Pure Corrosion and Abrasion-corrosion in a Simulated Marine Environment*, Tribology in Industry, vol. 41, no. 3, pp. 394-400, 2019, doi: 10.24874/ti.2019.41.03.09

[20] H.K.D.H. Bhadeshia, L.-E. Svensson, *Modelling the evolution of microstructure in steel weld metal. Mathematical modelling of weld phenomena*, Institute of Materials, vol. 1, pp. 109-182, 1993.

[21] V. Krasmik, J. Schlattmann, *Experimental Investigation of the Friction and Wear Behaviour with an Adapted Ball on Prism Test Setup*, Tribology in Industry, vol. 37, no. 3, pp. 291-298, 2015.

[22] C. Guoqing, F. Xuesong, W. Yanhui, L. Shan, Z. Wenlong, *Microstructure and wear properties of nickel-based surfacing deposited by plasma transferred arc welding*, Surface and Coatings Technology, vol. 228, no. 1, pp. S276-S282, 2013, doi: 10.1016/j.surfcoat.2012.05.125